Identification expérimentale de modèle réduit par MIM pour la prédiction de température dans des ruches vides.

Experiment-based Reduced Order Model by MIM applied to empty beehives for temperature prediction.

Manuel GIRAULT[1], Anna DUPLEIX[2], Anne LAVALETTE[2], Delphine JULLIEN[3], Emmanuel RUFFIO[2*]

[1]Institut PPRIME, UPR 3346 CNRS, ISAE-ENSMA, Université de Poitiers, Téléport 2, 1 avenue Clément ADER, BP 40109, F-86961 Futuroscope Chasseneuil, (France)
[2]AltRD, Co-actions Company, 46-48 rue Ferdinand Buisson, 33130 Begles (France)
[3]LMGC, Univ Montpellier, 163 rue Auguste Broussonnet, CC048, 34090 Montpellier (France)
[*](Corresponding author: emmanuel.ruffio@alt-rd.com)

Résumé – La surveillance à distance des ruches repose sur des systèmes embarqués connectés qui mesurent continuellement la masse de la ruche. La température est parfois mesurée mais peu d'algorithmes existent pour l'exploiter. Dans ce travail, des mesures de température obtenues sur une ruche vide sont utilisées pour identifier un modèle réduit par MIM. Les conditions météorologiques locales sont utilisées comme données d'entrée du modèle. Le modèle réduit est ensuite testé sur les jours suivants en comparant les températures simulées aux températures mesurées.

Abstract – Beehive monitoring systems rely on connected embedded systems which measure beehive weight variations. Temperature is sometimes monitored but few developments are done to implement algorithms to exploit it. In this work, temperature measurements in an empty hive are used to identify a reduced-order model using MIM. Local weather conditions are measured and used as model input. The model is then tested over the following days by comparing simulated and measured temperatures.

Nomenclature

C_p	specific heat capacity, J.kg^{-1}.K^{-1}
m	order of the model
N_{obs}	number of observable temperature sensors
N_t^{ident}	number of measures per sensor
N_f	number of sub-boundaries
h	heat transfer coefficient, W.m^{-2}.K^{-1}
t	time, s
T	temperature, K
v	wind velocity, m.s^{-1}
x	generic point in spatial domain

Greek symbols

φ	irradiance, Lux
λ	thermal conductivity, W.m^{-1}.K^{-1}
ρ	density, kg.m^{-3}
σ	mean quadratic discrepancy

Index and exponent

amb	relative to ambient
c	convective
ident	relative to ROM identification
r	radiative
valid	relative to ROM validation

1. Introduction

Beekeepers are facing environmental challenges that threaten their profession [1], like varroa mite and Asian hornet infestation, extreme temperature events, variable floral resources, etc. These threats alter the normal behavior and the health of bee colonies which

https://doi.org/10.25855/SFT2025-087

leads to financial loss due to lower productivity. Various companies have developed wireless devices to help beekeepers to keep track of their colonies and to reduce unnecessary trips by monitoring the weight and the temperature of the hive. Weight data are easier to analyze since they are closely related to bee colony activities [2]**:** (1) the flow of bees going in and out of the hive (few kilograms per day), (2) the increasing amount of resources (honey…) stored in hive frames, (3) the beekeeper activities (like addition of supers or thermal insulation), etc.

Temperature variations are more challenging to understand since they are highly sensitive to several factors independent of colony activities, like (1) local weather conditions, (2) close environment properties (surroundings objects, reliefs, ground type), (3) beehive materials and coatings, (4) beehive configuration (feeders, supers, closed/opened floor, vent holes, etc.), and the last factor but not least: sensor locations.

During high temperature events, some beekeepers had experienced wax frames collapsing in their hive. The melting temperature of pure bee wax is around 65°C. In south of France, the Dadant hive roof temperature reaches 70°C to 90°C on a daily basis. Experiments were carried out to measure the effect of paints [3] on the hive temperature.

To prevent overheating or overcooling issues, this work investigates the use of reduced-order model (ROM) to simulate the temperature of an empty hive based on measurements of the local weather. This is a preliminary work for a future goal which consists in implementing an algorithm able to predict the temperatures in an inhabited hive several days in advance using a weather scenario. The model is identified using the Modal Identification Method (MIM), from temperature measurements. Experiment-based ROMs are promising for embedded applications. The key advantage is indeed to avoid having to specify hive geometry and material properties which are hive-specific and, for some of them, time-varying. For example, the hive geometry depends on season and weather conditions since beekeepers add equipment to the hive to fulfill the colony needs. In these conditions, standard modeling approach is hardly feasible. Moreover, although MIM was used in several types of problems for building linear and nonlinear ROMs from measured data (see [4] for instance), this is the first time MIM is used to build Linear Time-Varying (LTV) ROMs, for which the coefficients are time-dependent.

After the description of the experimental setup in section 2, the local heat transfer equations and the corresponding assumptions used to define the ROM are introduced in section 3. The mathematical development to get the LTV ROM equations is then presented (section 4). Section 5 focuses on ROM identification using an optimization algorithm. Finally, a ROM is identified with 9 days of data provided by an instrumented hive. The last 2 days of available data are used for validation by comparing ROM simulations and actual measurements.

2. Description of the experiment

The experimental apiary (Figure 1) is located in Cevennes (France). This study focuses on the very common hive called Dadant. It is a frame-based hive which has proven to be very convenient to use by decades of beekeeping. Like most hives, Dadant hives are made of several parts that can be stacked up depending on the season and the needs. For example, if bees are running out of space to store nectar/honey/larvae/etc…, beekeepers add “honey supers” above the hive body. In this work, no additional part is installed.

This Dadant hive is made of chestnut wood and has a galvanized steel roof. To monitor the roof temperature, 5 temperature sensors (TC74 chip, 8 bits) are screwed at the center of each face (Figure 2). There are 4 other temperature sensors (NCT75 chip, 12 bits) installed in the hive: (1) on the upper side of the overframe, at about 2cm below the roof, (2) at the top of the

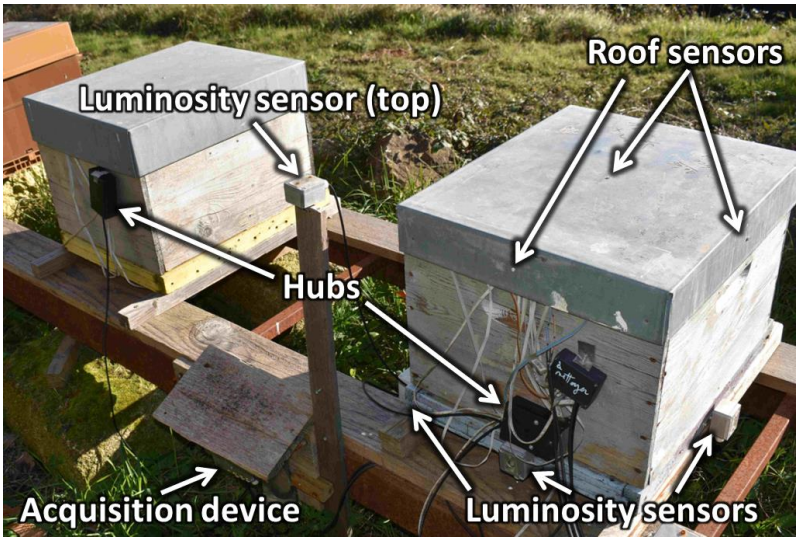

Figure 1*: Experimental apiary located in Cévennes (France) with instrumented Dadant hives facing south*

Figure 2: *Position of the 9 sensors in the Dadant hive*

body part, (3) at the bottom of the body part and (4) outside the hive at about 1cm below the bottom face. The roof sensors are the most reliable thanks to the good thermal contact with the steel. It is not very clear what the other sensors are actually measuring but it would be difficult to do anything better in real beekeeping conditions, i.e. with a colony inside and the need to move the hive regularly. Radiation heat transfers induce measurement bias, especially for the overframe sensor, but these effects are out of the scope of this paper.

Local weather conditions are monitored using several sensors. The air temperature sensor (HIH8121 chip, 14 bits) is installed inside a radiative shield. Wind speed and direction are given by the Sparkfun weather sensor. The incoming solar radiation on each face of the hive is measured using 6 ambient light sensors (VEML7700, 14bits, 0-10^5 Lux) (Figure 1). The wavelength sensitivity window is 500-900 nm.

All sensors are integrated chips with response time lower than 1 min. An inter-calibration was carried out to reduce their biases. The acquisition system was designed and implemented by AltRD using an AVR microcontroller. The acquisition frequency is 1 sample/min except for the wind data which are acquired every 2 seconds and averaged over 1 minute.

3. Local governing heat transfer equations

Let us call Ω the 3D-domain corresponding to the beehive and Γ its boundary. Heat transfer across the walls and inside the beehive is assumed as heat conduction in a heterogeneous medium, with convective and radiative boundary conditions. The energy equation thus writes:

$$\frac{\partial T}{\partial t}(x,t) = \frac{1}{(\rho C_p)(x)}\vec{\nabla}.\left(\lambda(x)\vec{\nabla}T(x,t)\right) \qquad (1)$$

$T(x,t)$ is the temperature at point $x \in \Omega$ and time t. Both the volumetric heat capacity ρC_p and thermal conductivity λ are non-uniform, thus taking account of the different materials constituting the beehive. The boundary Γ is divided into N_f sub-boundaries $\Gamma_j, j \in \{1, \dots, N_f\}$. $N_f = 6$ for the considered beehive. Let us note $\vec{n}$ the local normal outward unit vector to the boundary. For each sub-boundary Γ_j, the boundary condition is written as follows:

$$\lambda(x)\vec{\nabla}T.\vec{n} = f_j(x)\varphi_j(t) + \left(h_{c,j}(x,t) + h_{r,j}(x)\right)\left(T_{amb,j}(t) - T(x,t)\right) \qquad (2)$$

The heat flux density $f_j(x)\varphi_j(t)$ (W.m^{-2}) due to incoming solar radiation on Γ_j is the product of the time-varying irradiance $\varphi_j(t)$ (Lux) by a spatial distribution $f_j(x)$ (W.m^{-2}.Lux^{-1}). $T_{amb,j}(t)$ is the ambient temperature along Γ_j. The convection coefficient distribution $h_{c,j}(x,t)$ between Γ_j and the surrounding environment is assumed to depend on the time-varying velocity of wind surrounding the beehive, according to the empirical correlation:

$$h_{c,j}(x,t) = h_{nat,j}(x) + b_j(x)v(t) \tag{3}$$

where $h_{nat,j}(x)$ is the natural convection coefficient distribution along Γ_j, $v(t)$ is the wind velocity, identical along all sub-boundaries, and $b_j(x)$ is a coefficient distribution specific to Γ_j. Radiative heat transfers are linearized through a heat radiation coefficient $h_{r,j}(x)$.

4. Linear Time-Varying Reduced-Order Model

We aim at building a ROM able to compute temperatures at chosen locations, as functions of irradiances $\varphi_j(t), j \in \{1, \dots, N_f\}$, ambient temperatures $T_{amb,j}(t)$ and wind velocity $v(t)$.

4.1 Approximation of temperature

As in many model reduction methods, the variable, here temperature, is written as:

$$T(x,t) \approx \sum_{i=1}^{m} \phi_i(x)a_i(t) \tag{4}$$

where m is "small" (lower than 10) and the $\phi_i(x), i \in \{1, \dots, m\}$, are a truncation of an orthonormal basis of the Hilbert space formed by the space $\mathcal{L}_2(\Omega)$ of square integrable functions on Ω equipped with the inner product $\langle \cdot,\cdot \rangle_{\rho C_p}$ weighted by the heat capacity $\rho C_p(x)$:

$$\langle f_1, f_2 \rangle_{\rho C_p} = \int_{\Omega} \rho C_p f_1 f_2 d\Omega \tag{5}$$

4.2 Galerkin projection of energy equation

Calling $\mathcal{R}(x,t)$ the residue of equation (1), the Galerkin projection using the weighted inner product (5) writes:

$$\langle \mathcal{R}, \phi_k \rangle_{\rho C_p} = \underbrace{\int_{\Omega} \rho C_p \frac{\partial T}{\partial t} \phi_k d\Omega}_{\mathcal{I}} - \underbrace{\int_{\Omega} \vec{\nabla}.\left(\lambda \vec{\nabla} T\right)\phi_k d\Omega}_{\mathcal{D}} = 0 \qquad \forall k \in \{1, \dots, m\} \tag{6}$$

The following steps, not detailed here, are then performed on equation (6):

- The diffusion term $\mathcal{D}$ is integrated by parts using $\int_\Omega f \vec{\nabla}.\vec{u} d\Omega = \int_\Gamma f \vec{u} \cdot \vec{n} d\Gamma - \int_\Omega \vec{u} \cdot \vec{\nabla} f d\Omega$, allowing to introduce boundary condition (2) and correlation (3) on sub-boundaries;
- Approximation (4) for $T(x,t)$ is injected in the remaining internal and boundary terms, taking account of orthonormality of functions $\phi_i(x), i \in \{1, \dots, m\}$ in the inertia term $\mathcal{I}$.

The diffusion matrix M_d with $[M_d]_{ki} = -\int_\Omega \lambda \vec{\nabla}\phi_i.\vec{\nabla}\phi_k d\Omega$ in the resulting set of m equations is real and symmetric. Let be $D \in \mathbb{R}^{m\times m}$ the diagonal matrix containing the eigenvalues of M_d and $P \in \mathbb{R}^{m\times m}$ the orthogonal matrix whose columns form a set of eigenvectors of M_d. One has $D = P^T M_d P$. The change of variable $a(t) = PX(t)$ yields the ROM:

$$\frac{dX(t)}{dt} = \left(D + A_{cr}(t)\right)X(t) + B(t)U(t) \tag{7}$$

With: $X(t) \in \mathbb{R}^m$ the state vector, solution of the ROM and $D \in \mathbb{R}^{m\times m}$ a diagonal matrix.

$A_{cr}(t) = A_h + v(t)A_b$, where matrices $A_h \in \mathbb{R}^{m\times m}$ and $A_b \in \mathbb{R}^{m\times m}$ are symmetric.
$B(t) = [B_{cr}(t) \quad B_\varphi] \in \mathbb{R}^{m\times 2N_f}$, where $B_{cr}(t) \in \mathbb{R}^{m\times N_f}$ and $B_\varphi \in \mathbb{R}^{m\times N_f}$.
$B_{cr}(t) = \left[W_{cr,(1)}(t) \cdots W_{cr,(N_f)}(t)\right]$ with $W_{cr,(j)}(t) = W_{h,(j)} + v(t)W_{b,(j)},\ j \in \{1, \dots, N_f\}$
$W_{h,(j)} \in \mathbb{R}^m,\ j \in \{1, \dots, N_f\}$, and $W_{b,(j)} \in \mathbb{R}^m,\ j \in \{1, \dots, N_f\}$, are vectors.
$U(t) = \begin{bmatrix} T_{amb}(t) \\ \varphi(t) \end{bmatrix} \in \mathbb{R}^{2N_f}$, where vectors $T_{amb}(t) \in \mathbb{R}^{N_f}$ and $\varphi(t) \in \mathbb{R}^{N_f}$ gather the $T_{amb,j}(t)$ and the $\varphi_j(t), j \in \{1, \dots, N_f\}$, respectively.

The ROM (7) is a Linear-Time Varying (LTV) model because state matrix $D + A_{cr}(t)$ and input matrix $B(t)$ depend on time t through wind velocity $v(t)$.

The following simplified case is considered: the ambient temperature for each face of the hive is the same and equal to $T_{air}(t)$ except for the bottom face whose ambient temperature is the measured temperature $T_{below}(t)$, i.e. along the $\Gamma_j, j \in \{1, \dots, N_f - 1\}$, $T_{amb,j}(t)$ are identical, equal to $T_{air}(t)$, and along Γ_{N_f} (bottom face), $T_{amb,N_f}(t) = T_{below}(t)$. Thus:

$$U(t) = \begin{bmatrix} T_{air}(t) \\ T_{below}(t) \\ \varphi(t) \end{bmatrix} \in \mathbb{R}^{2+N_f} \text{ and } B_{cr}(t) = [W_{ah} + v(t)W_{ab} \quad W_{bh} + v(t)W_{bb}] \in \mathbb{R}^{m\times 2}$$

4.3 Selection of observable temperatures

We are interested in some observable temperatures at chosen locations $x_j,\ j \in \{1, \dots, N_{obs}\}$ gathered in vector $T_{obs} \in \mathbb{R}^{N_{obs}}$. Using the temperature approximation (4) and defining matrix $M_{obs} \in \mathbb{R}^{N_{obs}\times m}$ such as $[M_{obs}]_{ji} = \phi_i(x_j) \quad \forall j \in \{1, \dots, N_{obs}\}, \forall i \in \{1, \dots, m\}$, one gets:

$$[T_{obs}]_j(t) = T(x_j, t) = \sum_{i=1}^{m} \phi_i(x_j) a_i(t) = \sum_{i=1}^{m} [M_{obs}]_{ji} a_i(t) \quad j \in \{1, \dots, N_{obs}\}$$

which also writes in matrix form: $T_{obs}(t) = M_{obs}a(t)$. Injecting $a(t) = PX(t)$ in the above equation and defining $H = M_{obs}P \in \mathbb{R}^{N_{obs}\times m}$ leads to:

$$T_{obs}(t) = HX(t) \tag{8}$$

5. ROMs construction: identification procedure

The LTV ROM is composed of both equations (7) and (8). Matrices and vectors of the ROM, namely $D, A_h, A_b, W_{ah}, W_{ab}, W_{bh}, W_{bb}, B_\varphi$ and H, depend, as the case may be, on distributions $\lambda(x)$ and $f_j(x), h_{r,j}(x), h_{nat,j}(x), b_j(x), j \in \{1, \dots, N_f\}$, which are of course difficult to know accurately. They also depend on functions $\phi_i(x), i \in \{1, \dots, m\}$. Although these could be obtained from POD for instance, their computation would require 3D temperature snapshots. In the MIM framework, the literal expressions of constitutive matrices and vectors of the ROM are not used. Their components are identified through a parameter estimation problem, thus avoiding the need to know the previously mentioned distributions as well as functions $\phi_i(x)$. Because the initial thermal state does not correspond to a steady regime, the components of the initial state vector $X(t_{init})$ are additional unknowns. Except for components of matrix H, unknown parameters are gathered into a vector called θ. All parameters are identified through the minimization of the quadratic functional $\mathcal{J}_{ident}^{(m)}(\theta, H)$:

$$\mathcal{J}_{ident}^{(m)}(\theta, H) = \sum_{i=1}^{N_{obs}} \sum_{j=1}^{N_t^{ident}} \left([T_{obs}^{ROM}]_i(t_j, \theta, H) - [T_{obs}^{meas}]_i(t_j)\right)^2 \tag{9}$$

where T_{obs}^{ROM} is the vector of observed temperatures computed with the ROM and T_{obs}^{meas} is the vector of observed temperatures measured by the sensors installed on and in the beehive.

N_t^{ident} is the number of instants used in the ROM identification procedure. The mean quadratic discrepancy $\sigma_{ident}^{(m)}$ (in K) is used to assess the quality of the identified ROM:

$$\sigma_{ident}^{(m)} = \sqrt{\mathcal{J}_{ident}^{(m)}(\theta, H)/\left(N_{obs}N_t^{ident}\right)} \tag{10}$$

Equation (8) shows that the ROM output vector T_{obs} depends linearly on matrix H whereas equation (7) shows that it has nonlinear dependency on matrices and vectors whose components are gathered in θ. As a result, two types of optimization methods are used for the minimization of $\mathcal{J}_{ident}^{(m)}(\theta, H)$ through a two-step approach. A nonlinear iterative method is employed for the estimation of vector θ. A Particle Swarm Optimization (PSO) algorithm [5] has been used in the present work. At each iteration of the PSO algorithm and for all particles, state vector $X(t)$ is computed at all instants and matrix H (its transpose more precisely) is computed via Ordinary Least Squares (OLS) using measured temperatures. Both optimization methods are briefly described in [6], for instance. Starting with $m = 1$, ROMs are built successively by incrementing order m and minimizing corresponding functional $\mathcal{J}_{ident}^{(m)}(\theta, H)$. For $m = 1$, components of θ are randomly initialized. When identifying the order $m + 1$ ROM ($m \geq 1$), the components of θ in the order m ROM previously identified are used as initial guesses for the corresponding unknown components of θ in the order $m + 1$ ROM.

6. Results

Wind velocity $v(t)$, irradiances $\varphi_j(t)$, $j \in \{1, \dots, N_f\}$ and ambient temperatures T_{air} and T_{below} are respectively shown in Figure *3*, Figure *4* and Figure 5. Corresponding observable temperatures ("Roof", "Overframe", "Top", "Bottom", as well as "North", "South", "East" and "West" on roof) have also been measured. Thus N_{obs}= 8. Data have been recorded during a bit more than 11 days. A first part of data is used for ROMs construction, the remaining recorded days being employed for validation of ROMs simulations. It is necessary to use at least the first 9 days of recorded data to build ROMs able to give good simulations. This is in accordance with Figure *3*, which shows large variations of wind velocity (the quantity that makes the ROMs matrices $A_{cr}(t)$ and $B(t)$ varying with time) over the 9 first days. These 9 first days correspond to N_t^{ident} = 12188 instants. A series of ROMs of order 1 to 10 have been built. The number of ROM constitutive parameters (except the $N_{obs}m$ components of matrix H) is $N_{param} = m(m + 1) + m\left(6 + N_f\right)$ with N_f = 6 here. The mean quadratic discrepancy $\sigma_{ident}^{(m)}$ with respect to ROM order m is shown in Figure 6 (red curve). $\sigma_{ident}^{(m)}$ decreases monotonically with m, from about 2.70°C for order 1 ROM down to about 0.77°C for order 10 ROM.

For the simulation part (blue curve in Figure 6), the initial state X is given by the final state of the identification part and the environmental data are used as model input. The mean quadratic discrepancy $\sigma_{valid}^{(m)}$ is not as low as the identification part, and decreases up to order 3 only, before increasing. Thus, higher order ROMs, whose outputs values are closer to measured data in the ROMs identification phase, are not as good to simulate temperatures. Some of their constitutive parameters, identified through the MIM optimization procedure, are too much specific to the data used for construction: they do not bring much more improvement in the identification phase but induce large errors when the ROMs are used to simulate temperatures. Although it was expected for $\sigma_{valid}^{(m)}$ to be larger than $\sigma_{ident}^{(m)}$, the gap is quite large. However, the ROM of order 3 allows for quite satisfying simulations, with $\sigma_{valid}^{(m=3)}$=2.84°C compared to $\sigma_{ident}^{(m=3)}$=1.24°C. Temperatures on Roof, Overframe, Top and Bottom are shown respectively in Figure 7, Figure 8, Figure 9 and Figure 10, for the order 3

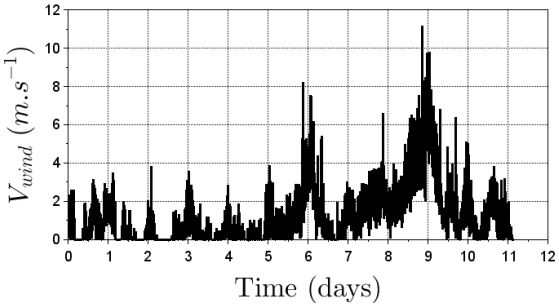

Figure 3: *Wind velocity*

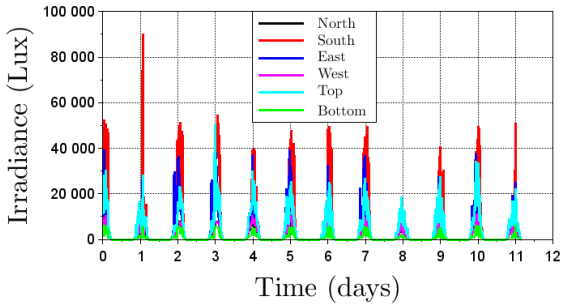

Figure 4: *Irradiances on the 6 faces*

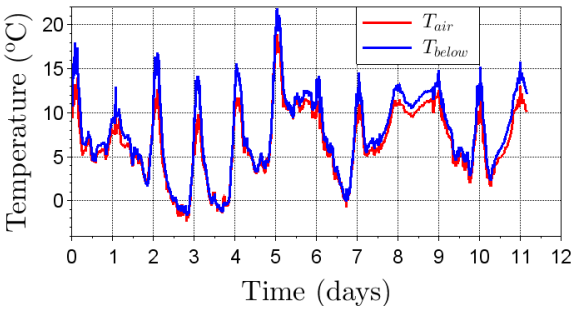

Figure 5: *Temperatures T_{air} and T_{below}*

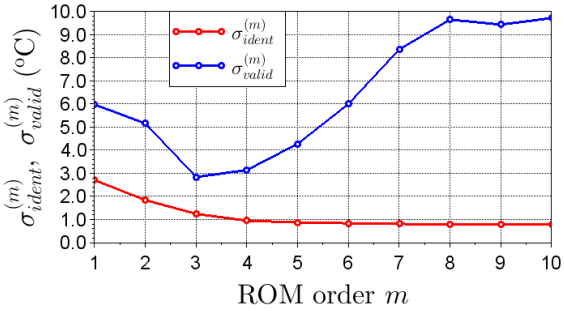

Figure 6: *Mean quadratic discrepancies between ROMs outputs and measured temperatures*

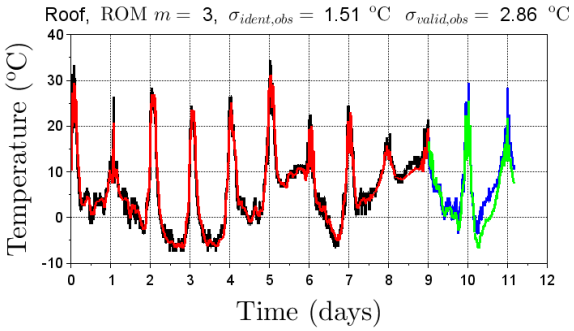

Figure 7: *Roof temperature: measured data and outputs of ROM of order 3*

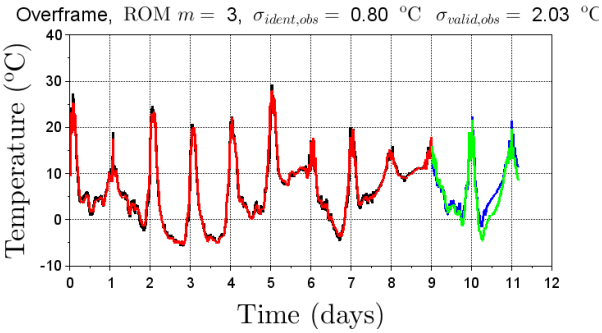

Figure 8: *Overframe temperature: measured data and outputs of ROM of order 3*

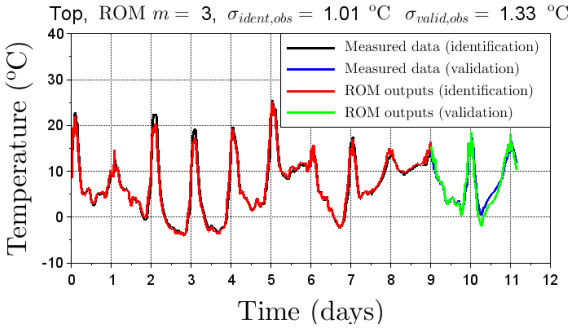

Figure 9: *Top temperature: measured data and outputs of ROM of order 3*

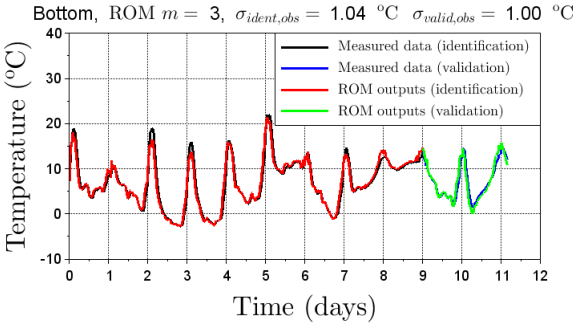

Figure 10: *Bottom temperature: measured data and outputs of ROM of order 3*

ROM (legend of Figure 9 and Figure 10 is also valid for Figure 7 and Figure 8). It should be noted that temperatures inside the hive (Top and Bottom), the most useful for the beekeepers, are accurately simulated with the order 3 ROM. This is confirmed by the mean quadratic discrepancies relative to each of these two specific temperatures: $\sigma_{valid,obs}^{(m=3)}$ is about 1°C, close to $\sigma_{ident,obs}^{(m=3)}$ (see values at top of Figure 9 and Figure 10).

7. Conclusion

The temperature values at various locations in a Dadant hive were measured for 11 days. The wind speed, the air temperature and the solar heat radiation on the 6 hive's faces were monitored as well. The first 9 days were used to train sequentially a set of 10 reduced-order model, i.e. one order after the other, from order 1 to 10. These models were derived from local heat transfer equation by applying a Galerkin projection. By increasing the order of the model, the number of unknown parameters that has to be estimated increases rapidly. During the identification stage, it was shown that the discrepancies between model outputs and measurements keep decreasing with the increasing order. For the simulation phase, the model had to simulate the hive temperatures of the last 2 days, given the ambient measurements (air, wind, solar radiation). The discrepancies were minimal for the model of order 3 but rise again up to order 10. This increase is probably due to the large number of unknown parameters (230 at order 10 compared to 48 at order 3) which increases instabilities if parameters are not estimated precisely enough. Indeed the data used for the identification are crucial since they must cover all the future operating conditions for the model. Nevertheless, this order 3 model succeeded in simulating in-hive temperatures with a discrepancy lower than 2°C but some errors up to 3°C were found on the roof.

Next development will consist in improving the simulation capability by using longer time series and in assessing the sensitivity of simulation quality to the number of sensors. For future use in beehives, it is indeed crucial to use as fewer sensors as possible. It would be useful to take account of the standard deviation of temperature measurements error to determine the order of the model. Taking account, in the model, of volumetric heat capacity variations with honey production and comings and goings of bees (their own mass and the mass of water they bring to cool their beehive), would be a long-term objective.

References

[1] P. de La Rúa, R. Jaffé, R. Dall'Olio, I. Muñoz, J. Serrano, Biodiversity, conservation and current threats to European honeybees, Apidologie, 40 (3) (2009), 10.1051/apido/2009027

[2] H. Hadjur, D. Ammar, L. Lefèvre. Toward an intelligent and efficient beehive: A survey of precision beekeeping systems and services, Computers and Electronics in Agriculture, Elsevier, 192, pp.1-16 (2022), 10.1016/j.compag.2021.106604

[3] A. Dupleix, A. Lavalette, E. Ruffio, C. Adolphe, Effets de différents revêtements sur la température au sein de la ruche, Technique Apicole, Abeille de France, 1119 Janvier (2024)

[4] M. Girault, E. Videcoq, Temperature regulation and tracking in a MIMO system with a mobile heat source by LQG control with a low order model, *Control Eng. Pract.*, 21-3 (2013), 333-349.

[5] M. Clerc, Particle Swarm Optimization, New-York: Wiley-ISTE, (2013)

[6] M. Girault, Q. Lin, N. Allanic, P. Mousseau, Thermo-rheological reduced order models for non-Newtonian fluid flows with power-law viscosity via the modal identification method, *Int. J. Heat Mass Transf.*, 203 (2023), 123692. 10.1016/j.ijheatmasstransfer.2022.123692.

Acknowledgements

This work was supported by the Better-B project, which has received funding from the European Union, the Swiss State Secretariat for Education, Research and Innovation (SERI) and UK Research and Innovation (UKRI) under the UK government's Horizon Europe funding guarantee (grant number 10068544). Views and opinions expressed are however those of the author(s) only and do not necessarily reflect those of the European Union, European Research Executive Agency (REA), SERI or UKRI. Neither the European Union nor the granting authorities can be held responsible for them.